

Cancer-associated mutants of RNA helicase DDX3X are defective in RNA-stimulated ATP hydrolysis

Leslie B. Epling^{1#}, Christy R. Grace^{1#}, Brandon R. Lowe^{2,3#}, Janet F. Partridge^{2,3*}, Eric J. Enemark^{1,3*}

¹Department of Structural Biology, St Jude Children's Research Hospital, 262 Danny Thomas Place, Mail Stop 311, Memphis, TN 38105, USA

²Department of Pathology, St Jude Children's Research Hospital, 262 Danny Thomas Place, Mail Stop 350, Memphis, TN 38105, USA

³Program in Biomedical Sciences, University of Tennessee Health Science Center, 858 Madison Ave., Memphis, TN 38163, USA

#These authors contributed equally to this work.

*To whom correspondence should be addressed.

Supplementary Materials

Figure S1. The domain architecture of DDX3X.

Figure S2. RNA-stimulated ATPase activity of DDX3X and its cancer-associated mutants.

Figure S3. Interdomain conformation of DDX3X D354V and the ATPase active site.

Figure S4. Stereoviews of electron density in the crystal structure of *HsDDX3X* (135-582) D354V.

Figure S5. A conserved phenylalanine of the ABL (see Figure S1b) projects into a hydrophobic pocket.

Figure S6. Structural similarity of DDX3X D1 and its ATP-binding Loop when comparing D1-only to D1-D2.

Figure S7. Stereoviews of electron density in the crystal structure of *HsDDX3X* (135-407).

Figure S8. DDX3X D1 interaction with nucleic acids in solution.

Figure S9. Electrophoretic mobility shift assay (EMSA) binding experiments for DDX3X and the cancer-associated mutants.

Figure S10. Phosphate positions in the DDX3X D354V crystal structure are similar to the positions of ssRNA backbone phosphates bound to Vasa [1] based on D1 alignment.

Figure S11. Evaluation of potential binding models of DDX3X D1 with dsRNA.

Figure S12. DDX3X complements growth temperature-sensitive phenotype in *ded1-1D5* cells.

Figure S13. Analysis of DDX3X complementation of thermosensitive *ded1-1D5* cells.

Table S1. Crystallographic statistics.

Table S2. Chemical Shift values for DDX3X domain D1 (in ppm) at 298 K.

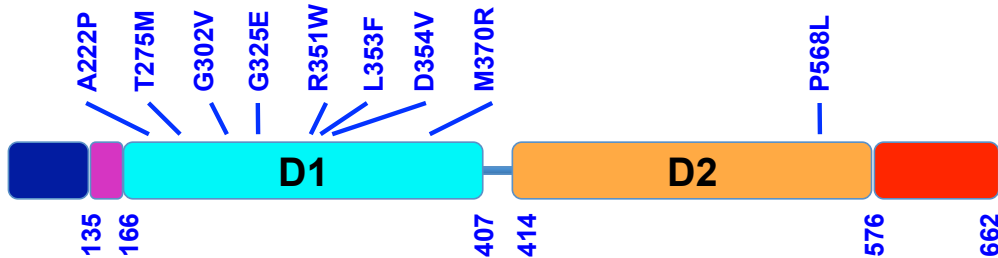
Table S3. Yeast strains used in this study.

Table S4. List of Plasmids used in this study

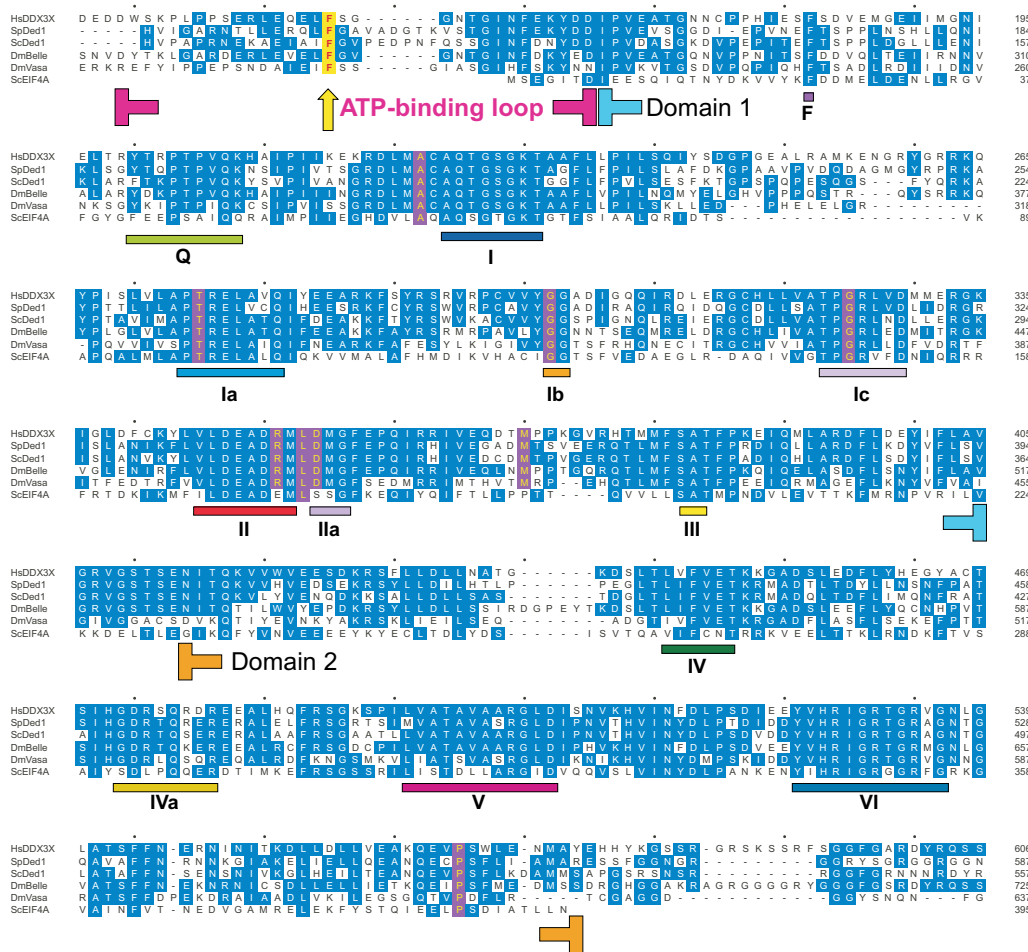
Supplementary References

(a)

DDX3X

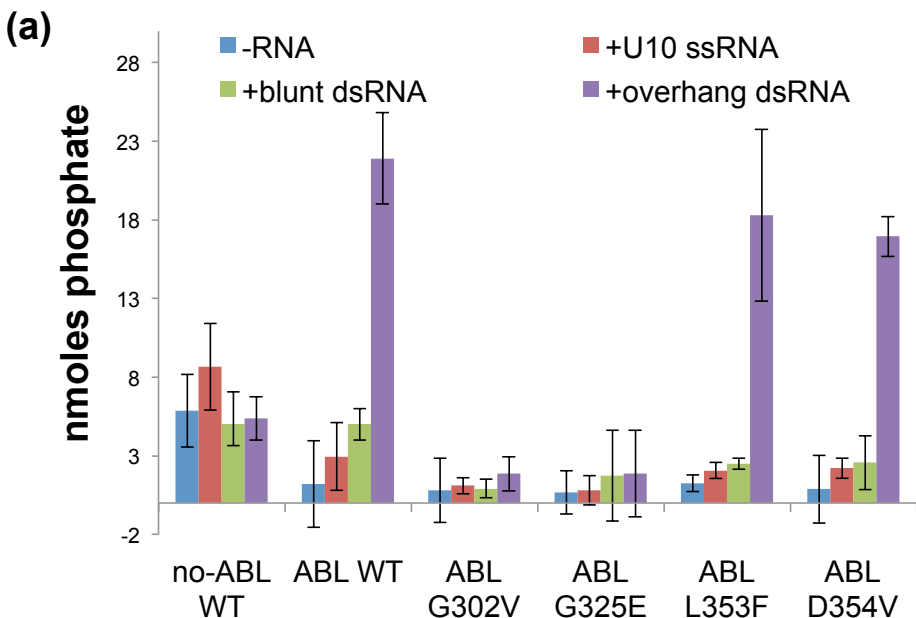


(b)

**Figure S1.** The domain architecture of DDX3X.

(a) Two RecA-like domains (cyan and light orange) flanked by N-and C-terminal extensions (dark blue and red, respectively). An N-terminal “ATP-binding loop” (ABL) described in this study is shown in magenta. The positions of cancer-associated mutations are noted above.

(b) Sequence alignment of DDX3X with close relatives Vasa and Ded1 and a canonical DEAD-box helicase, eIF4A. Residues identical to the consensus are shaded blue. The residues that are mutated in medulloblastoma or ALL are conserved among DDX3X, Ded1, and Vasa, and are shaded red. Helicase sequence motifs are noted below the alignment. A conserved phenylalanine identified in the ABL is shaded yellow.



(b)

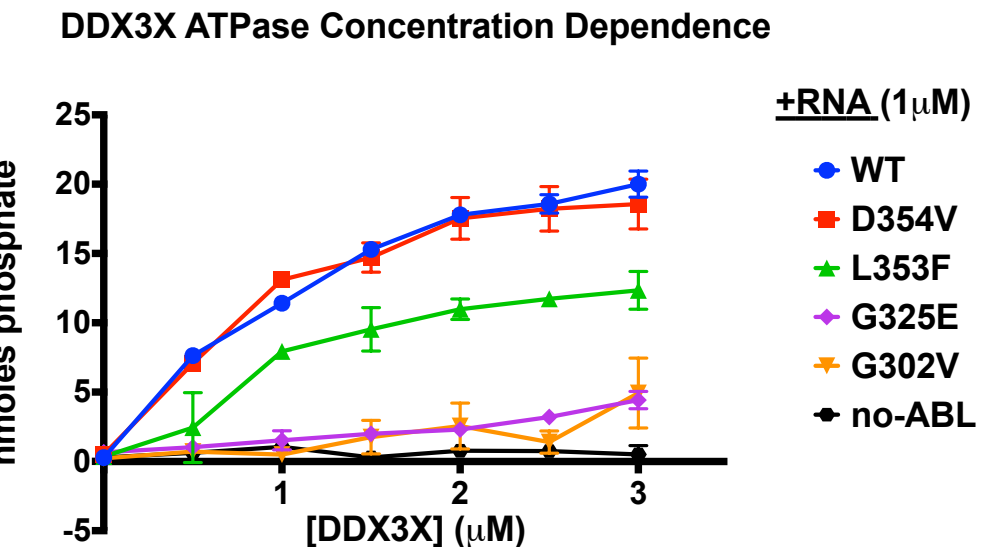


Figure S2. RNA-stimulated ATPase activity of DDX3X and its cancer-associated mutants.

(a) The RNA-stimulated ATPase activity of DDX3X requires the ABL. Without the ABL, DDX3X (168-582, “no-ABL”) exhibited a very low ATPase activity. With the ABL, DDX3X (135-582, “ABL”) wild-type, L353F, and D354V all showed significant ATPase activity in the presence of 5'-tailed duplex RNA (purple). The same proteins had a negligible ATPase activity in the absence of RNA (blue) or in the presence of ssRNA (red) or blunt duplex RNA (green). In contrast, the G302V and G325E mutants are defective in ATPase activity. The mean and standard deviations of three independent experiments after 60 minute incubation of 3 μ M DDX3X, 2 mM ATP, and 1 μ g RNA (if present) are shown.

(b) DDX3X concentration-dependent RNA-stimulated ATPase activity. The mean and standard deviations of two independent experiments after 30 minute incubation of varying concentration of DDX3X, 2 mM ATP, and 1 μ g of 5'-tailed duplex RNA (1 μ M duplex; purple in panel a) are shown. Successive mean datapoints are connected with linear segments. Wild-type and D354V show similar activity. G302V and G325E are severely defective. The construct lacking the ABL (“no-ABL”) shows no detectable activity.

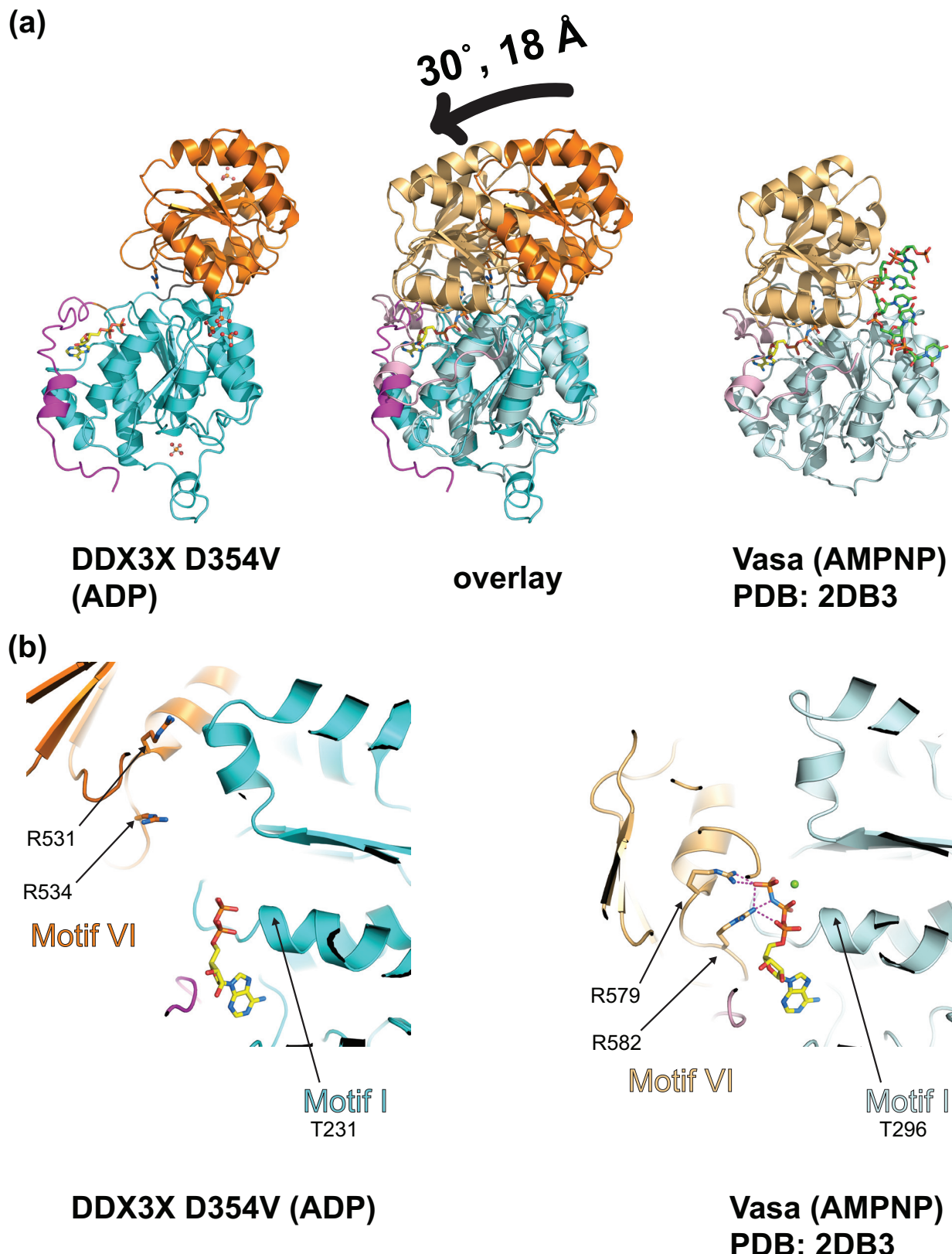
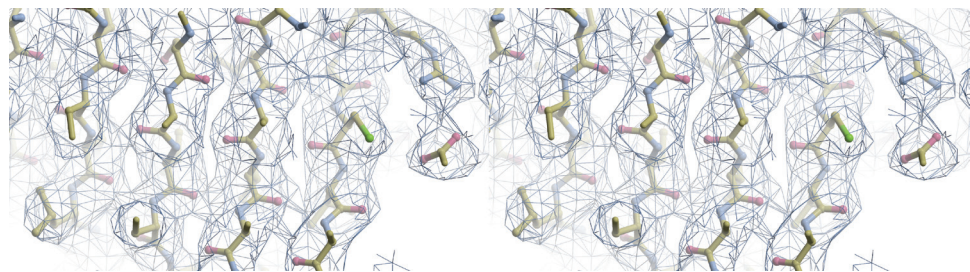


Figure S3. Interdomain conformation of DDX3X D354V and the ATPase active site.

(a) The crystallized conformation of DDX3X D354V (top left) is not in the “closed” conformation that was identified in a crystal structure of Vasa [1], top right, with bound RNA in green stick. A modest interdomain shift is required to yield a comparable closed conformation.

(b) ATP hydrolysis is not expected to occur in the crystallized “open” DDX3X conformation (left). The catalytically competent site of DDX3X is expected to closely resemble the conformation observed in the crystal structure of Vasa (right) [1].

(a) β -sheet region



(b) select phosphates, Motifs Ic, IVa

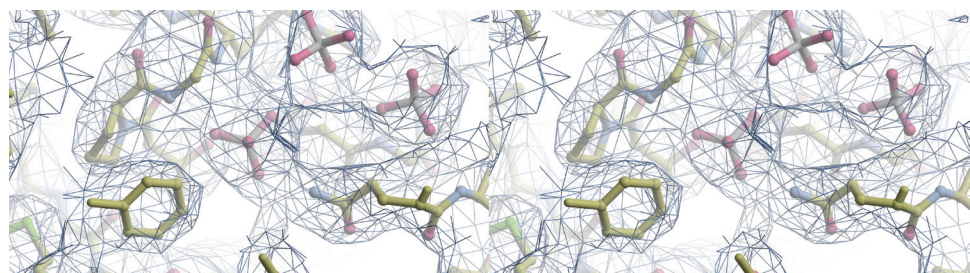
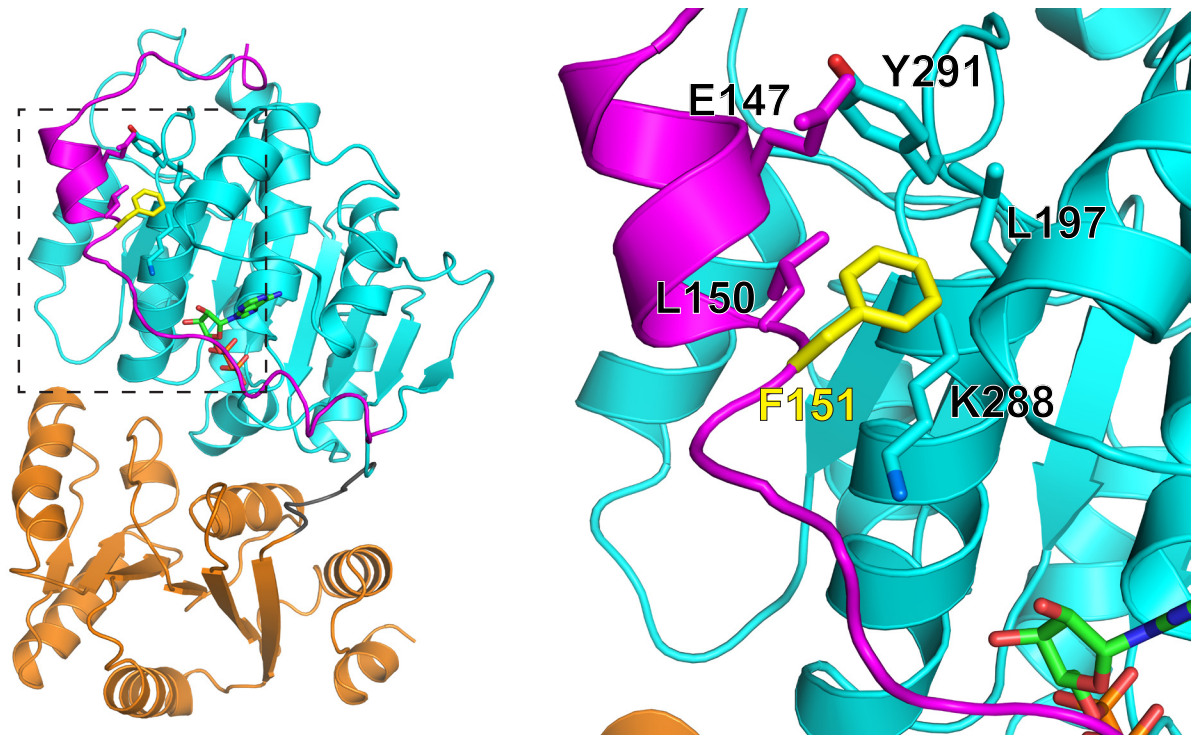


Figure S4. Stereoviews of electron density in the crystal structure of *HsDDX3X* (135-582) D354V.

(a) Narrow depth stereoview of the 2Fo-Fc electron density after the final round of refinement in a β -sheet region.

(b) Stereoview of the 2Fo-Fc electron density after the final round of refinement in the vicinity of select phosphate ions near G302 and G325.

(a) DDX3X D354V



(b) Vasa PDB: 2DB3

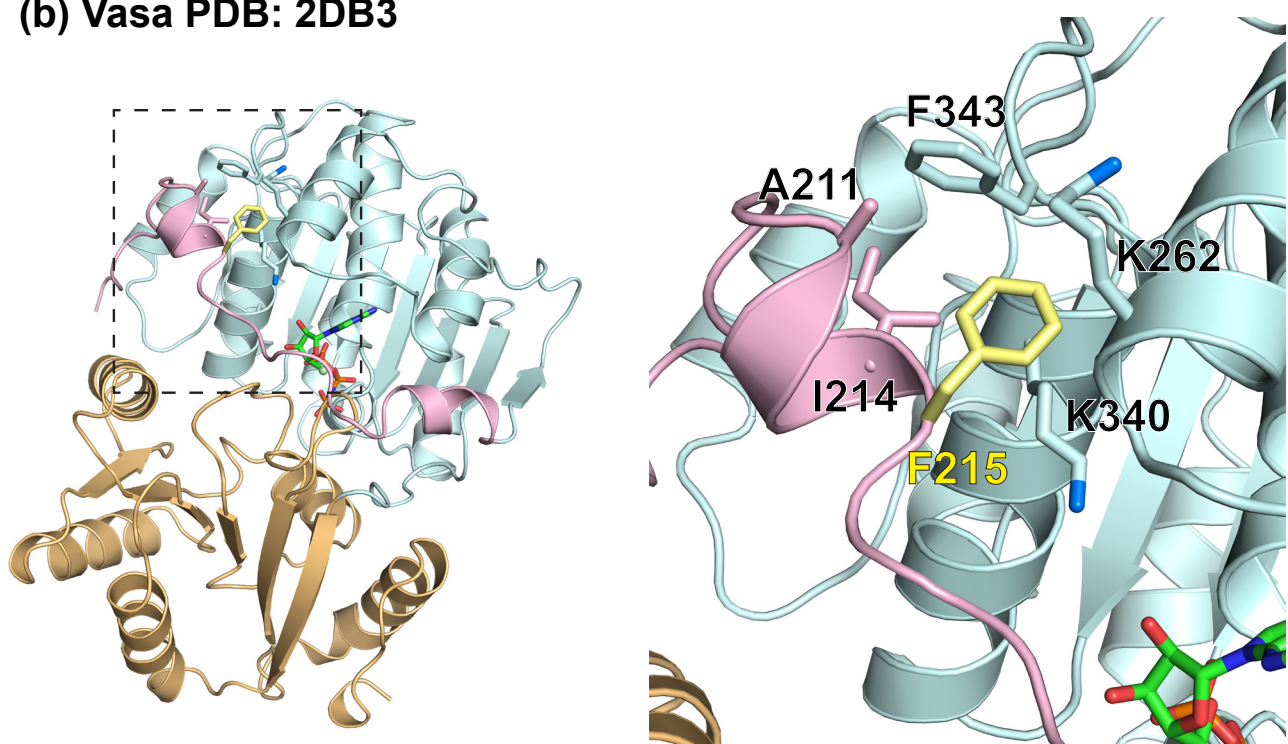
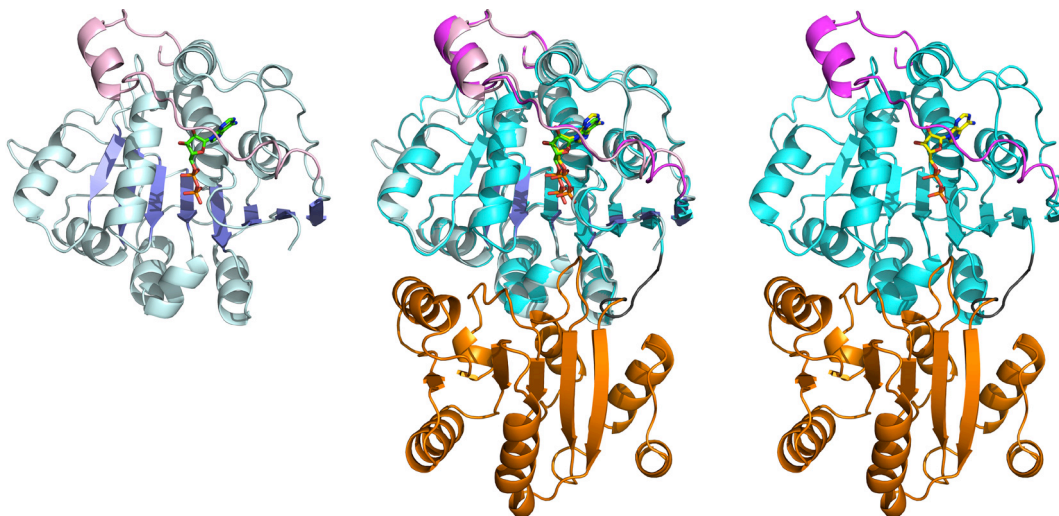


Figure S5. A conserved phenylalanine of the ABL (see Figure S1b) projects into a hydrophobic pocket.

(a) DDX3X F151 (yellow) on the ABL (magenta) projects into a pocket of D1 (cyan) detailed at right.

(b) Vasa [1] F215 (yellow) sits in a similar pocket to that of DDX3X.

(a)



DDX3X D1 (135-407)

Overlay

DDX3X D1-D2 (135-582)
D354V

(b)

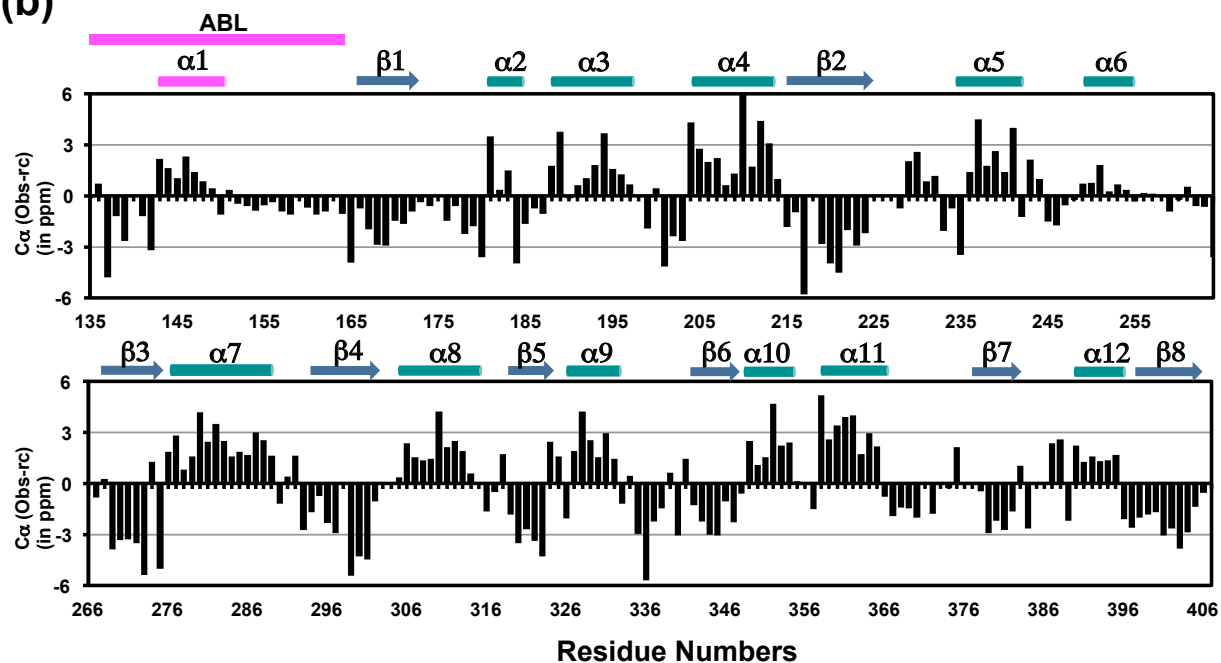
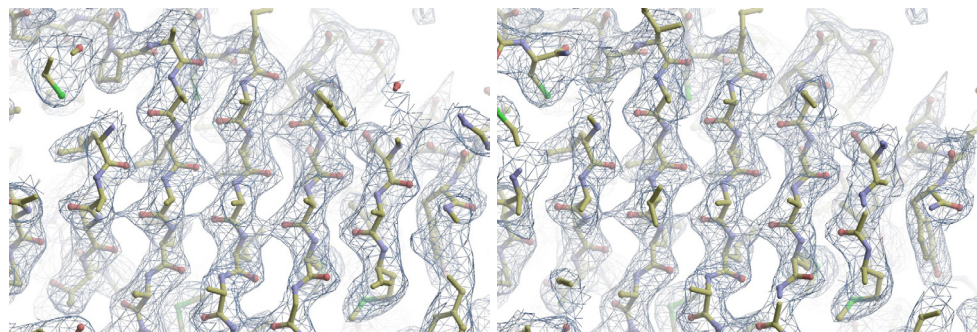


Figure S6. Structural similarity of DDX3X D1 and its ATP-binding Loop when comparing D1-only to D1-D2.

(a) The RMSD is 0.76 Å for all $\text{C}\alpha$ positions excluding residues 252-262, a poorly conserved loop that is structured differently.

(b) Chemical shift deviations plot for the C-alpha carbons. The secondary structure elements observed in the crystal structure (shown above) are also conserved in solution.

(a) β -sheet region



(b) ABL

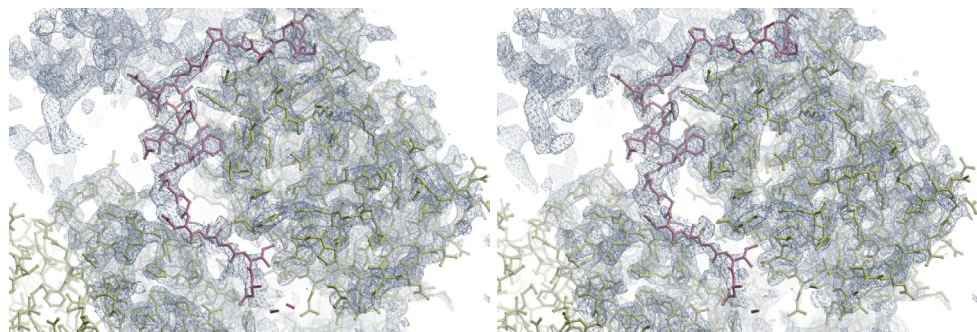


Figure S7. Stereoviews of electron density in the crystal structure of *HsDDX3X* (135-407).

(a) Narrow depth stereoview of the 2Fo-Fc electron density after the final round of refinement in the β -sheet region of one of the DDX3X D1 monomers.

(b) Stereoview of the 2Fo-Fc electron density after the final round of refinement in the vicinity of the ABL (magenta).

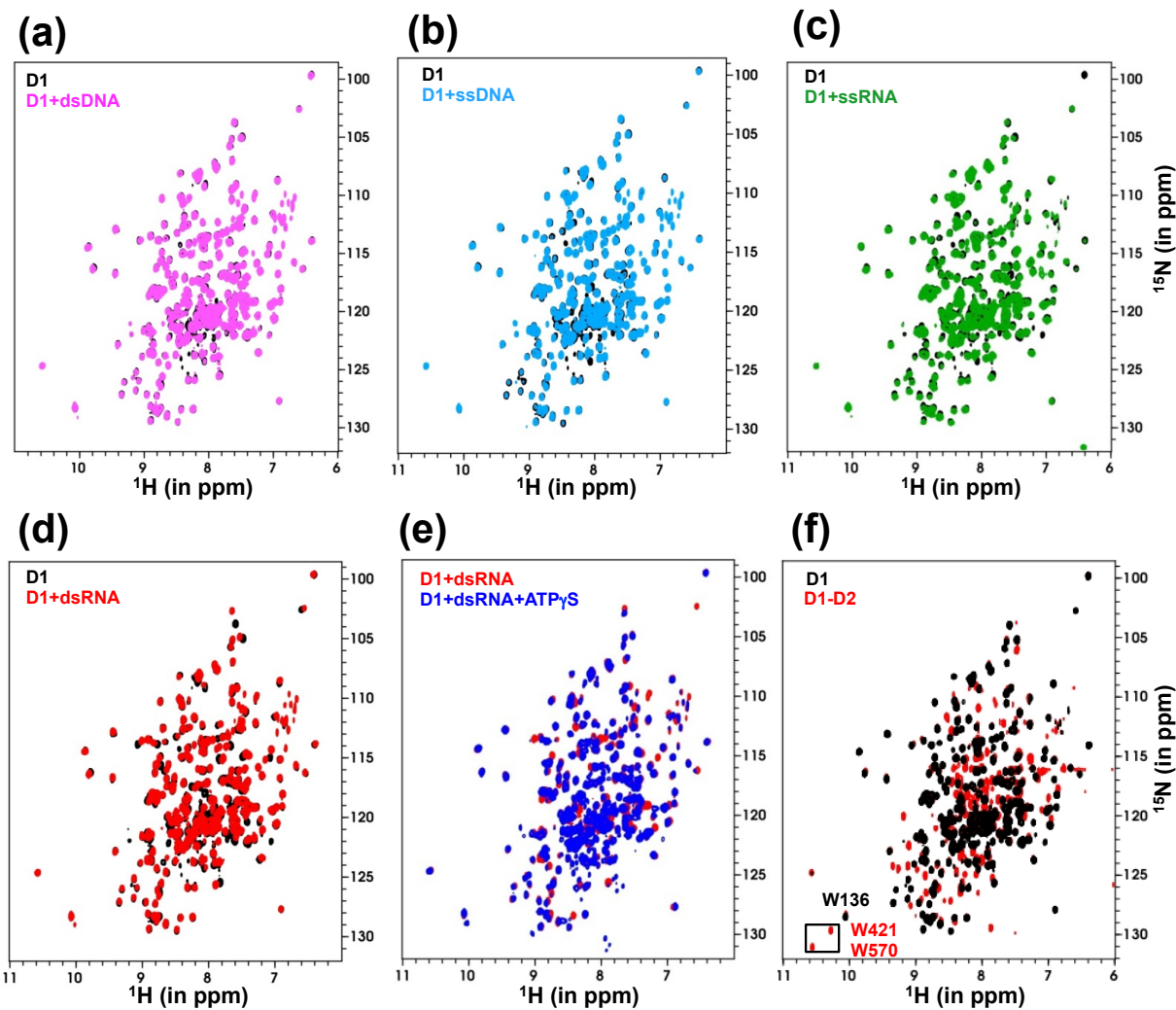


Figure S8. DDX3X D1 interaction with nucleic acids in solution.

Superposition of the $[{}^1\text{H}, {}^{15}\text{N}]$ TROSY spectra of DDX3X D1 (in black) with the same in the presence of the following nucleic acids in the molar ratio of 1:1.2:

(a) ds-DNA (in magenta)

(b) ss-DNA (in light blue)

(c) ss-RNA (in green)

(d) ds-RNA (in red)

(e) Superposition of the $[{}^1\text{H}, {}^{15}\text{N}]$ TROSY spectra of the D1-dsRNA complex (in red) shown in (D) with the same in the presence of 1:5 molar excess of ATP- γ S (in blue).

(f) Superposition of the $[{}^1\text{H}, {}^{15}\text{N}]$ TROSY spectra of DDX3X D1 (black, residues 135-407) and DDX3X D1-D2 (red, residues 135-582) reveals that most of the D1 chemical shifts are unchanged, indicating that D1 has a similar structure in the D1 and in the D1-D2 constructs. The side chains of the Trp residues in D1 (W136) and D2 (W421, W570) are marked for clarity.

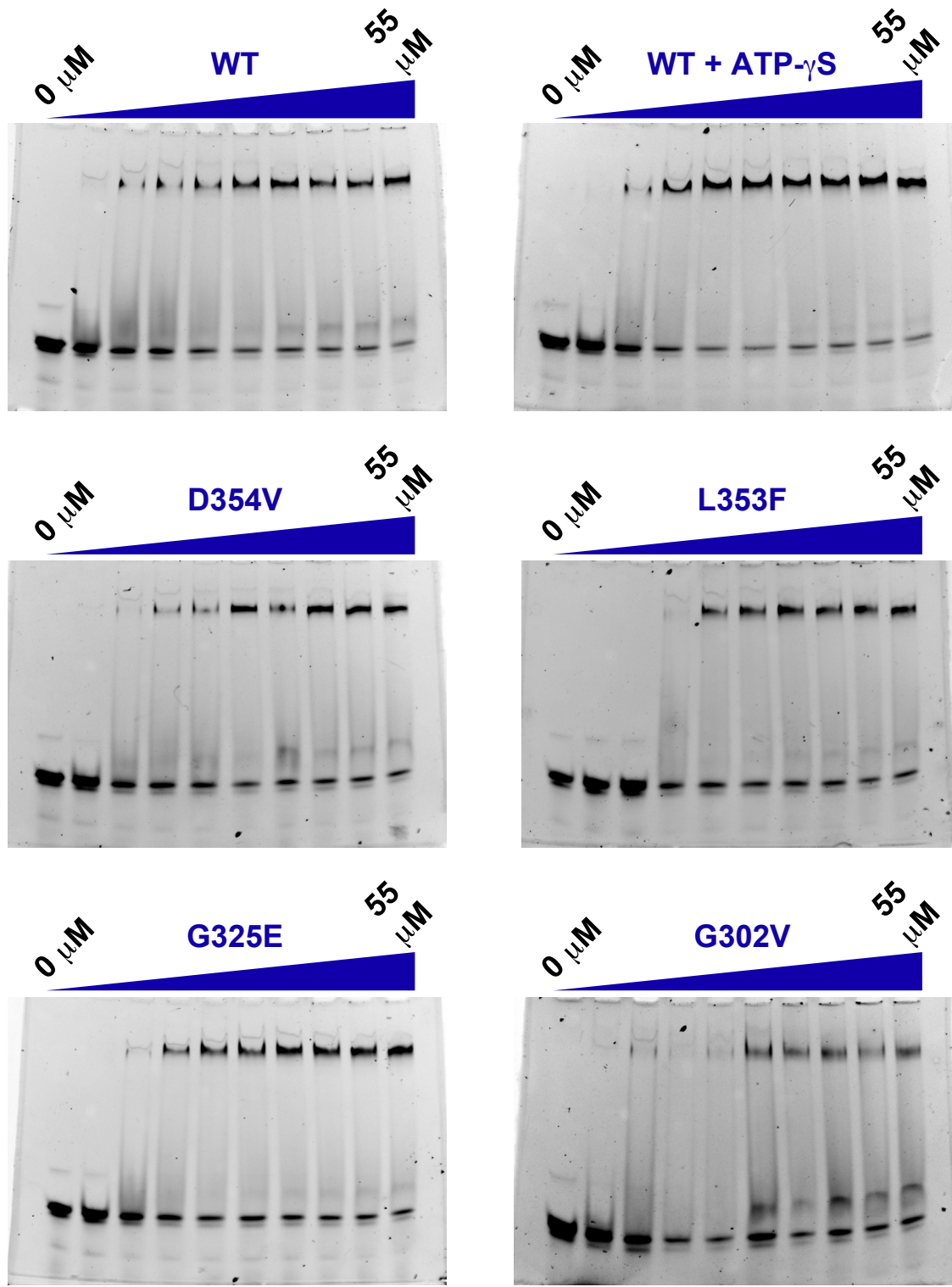
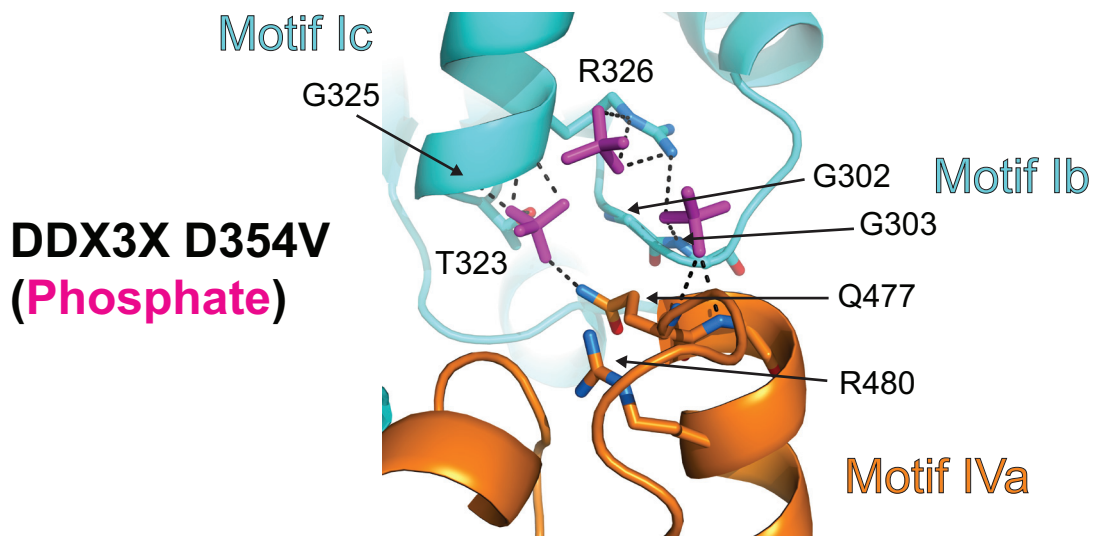


Figure S9. Electrophoretic mobility shift assay (EMSA) binding experiments for DDX3X and the cancer-associated mutants. Each protein was titrated from 0 to 55 μ M in the presence of 40 nM blunt duplex RNA substrate. The titration for wild-type DDX3X was also carried out in the presence of 1 mM ATP- γ S (top right). One representative gel of three independent experiments is shown for each titration.



overlay

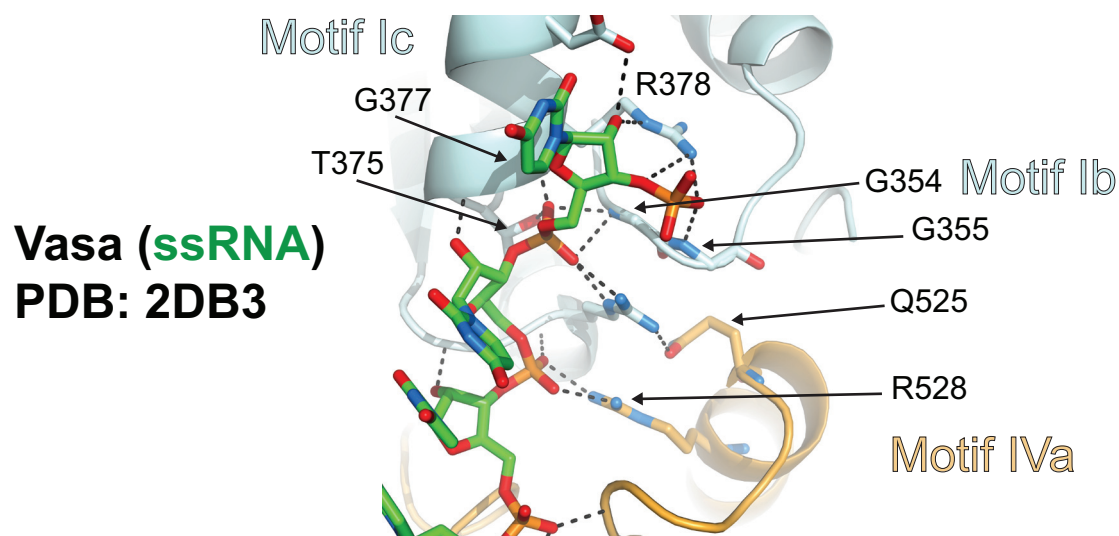
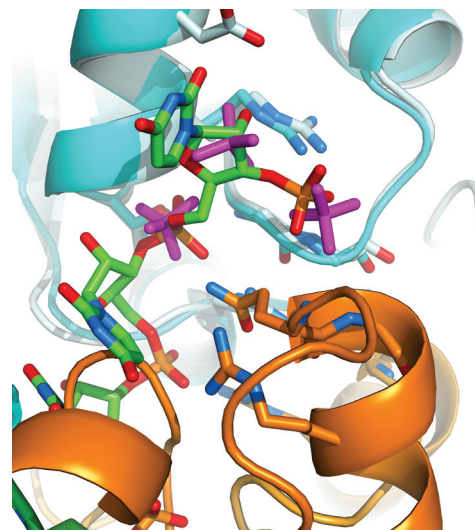


Figure S10. Phosphate positions in the DDX3X D354V crystal structure are similar to the positions of ssRNA backbone phosphates bound to Vasa [1] based on D1 alignment. For DDX3X (top) the phosphate ions

(magenta) are bound to residues of motif Ib and motif Ic, including residues G302 and G325, which have mutants associated with medulloblastoma. In the closed conformation of Vasa ([1], bottom), equivalent residues of D1 (motif Ib and motif Ic) bind two RNA (green stick) phosphates in very similar positions (middle).

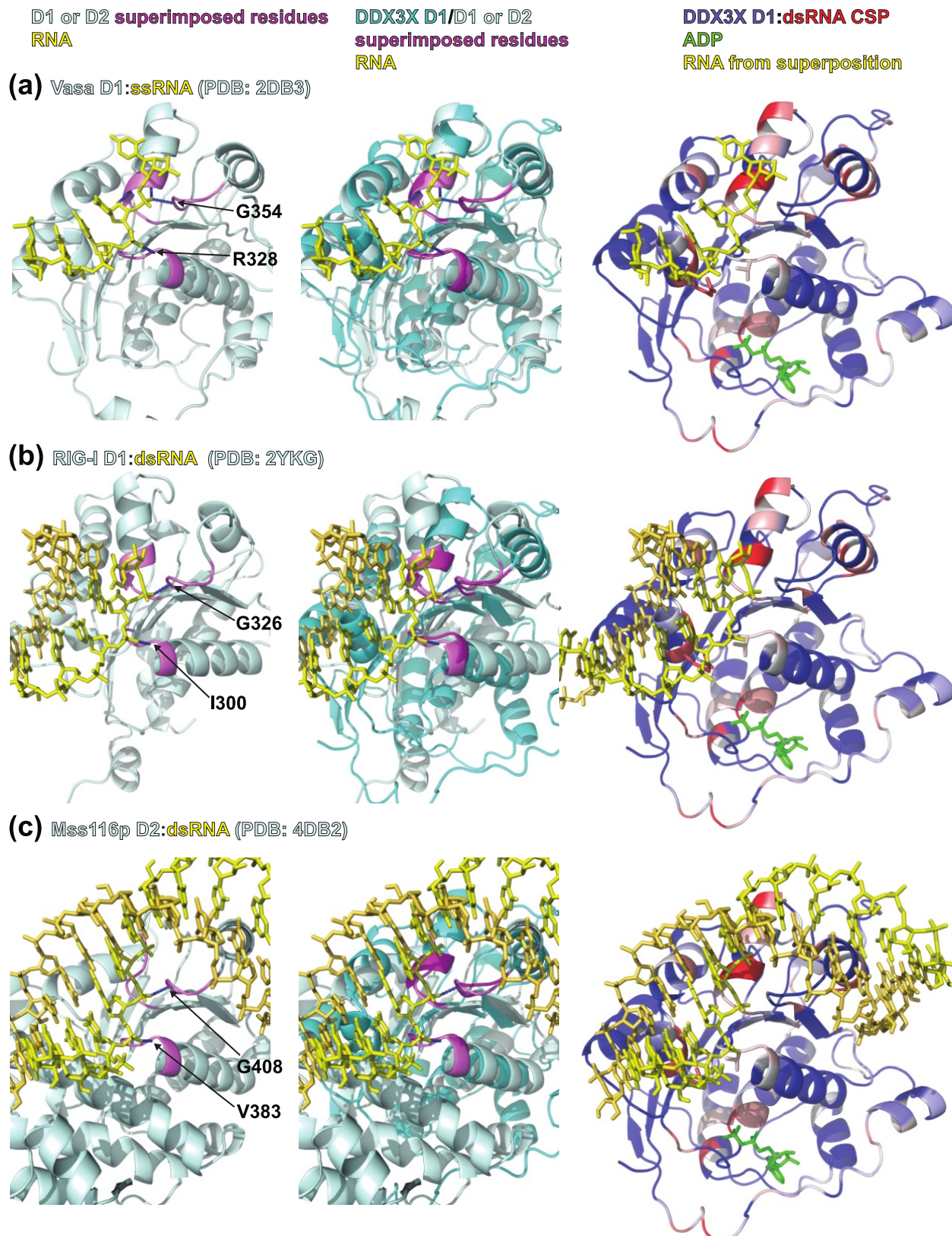


Figure S11. Evaluation of potential binding models of DDX3X D1 with dsRNA. Alignments were based on three conserved RNA-binding motifs that showed consistent interactions of main-chain amides with adjacent phosphates on the RNA backbone. The main-chain residues correspond to DDX3X R276 and G302. The

range of DDX3X D1 CSP upon binding dsRNA is shown in color ramp from blue (negligible CSP) to red (maximum CSP).

- (a) Superposition of the D1-portion of the Vasa:ssRNA structure (PDB: 2DB3) [1].
- (b) Superposition of the D1-portion of the RIG-I:dsRNA structure (PDB: 2YKG) [2].
- (c) Superposition of the Mss116p D2:dsRNA structure (PDB: 4DB2) [3].

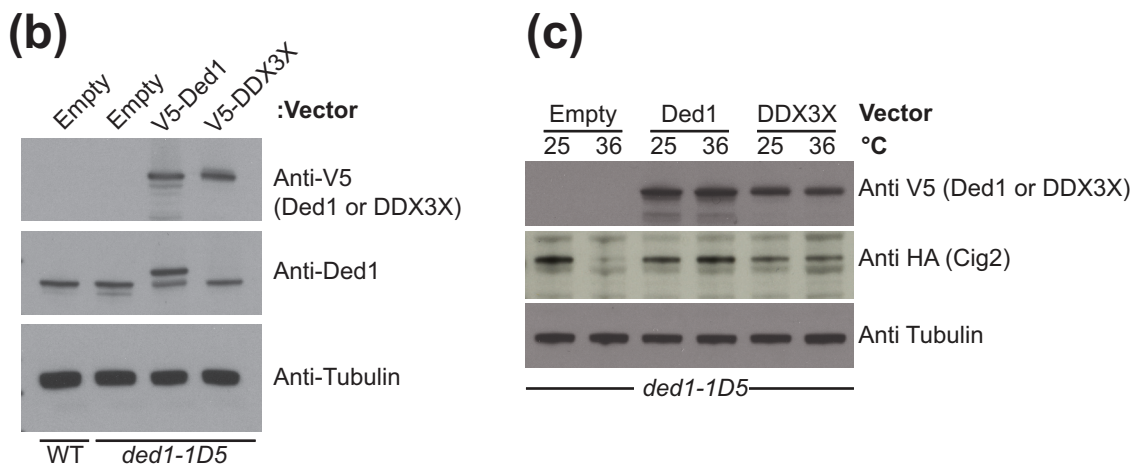
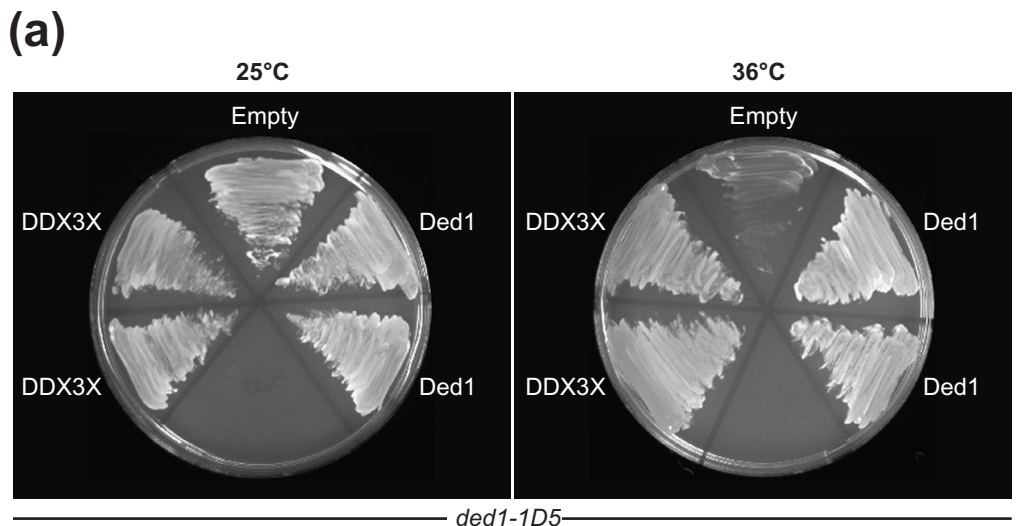


Figure S12. DDX3X complements growth temperature-sensitive phenotype in *ded1-1D5* cells.

(a) The temperature-sensitive growth defect of the *ded1-1D5* allele in *S. pombe* is rescued by wild-type DDX3X (left) or wild-type Ded1 (right) expression plasmids.

(b) Expression levels for DDX3X and Ded1 were less than 2-fold over endogenous Ded1 levels based upon comparison of Western blots against the V5 epitope tag and against Ded1.

(c) The temperature-sensitive growth defect correlates with a reduction in Cig2 expression at the restrictive temperature. Complementation by wild-type DDX3X or Ded1 restores Cig2 expression.

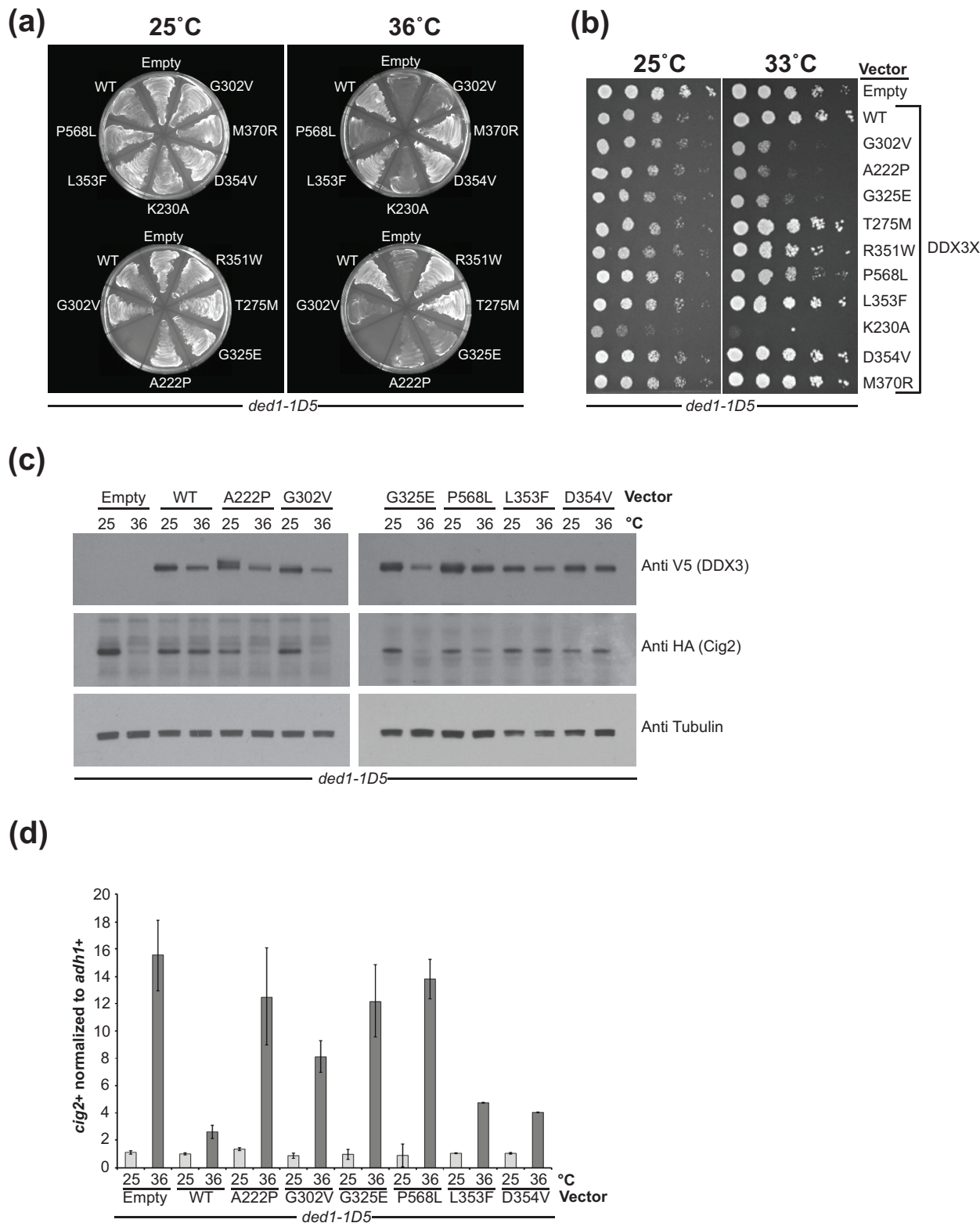


Figure S13. Analysis of DDX3X complementation of thermosensitive *ded1-D5* cells.

(a) Wild-type DDX3X complements the temperature-sensitivity of the *ded1-1D5* mutant whereas *ded1-1D5* strains expressing the medulloblastoma-associated mutants A222P, G302V, G325E, P568L, and the Walker-A mutant K230A exhibit temperature dependent growth defects.

(b) *ded1-1D5* strains expressing the DDX3X mutants were examined at an intermediate temperature (33°C) in a serial dilution assay to show the degree of defect. The Walker-A mutant, K230A, was the most defective. Growth of strains expressing the DDX3X mutants A222P, G302V, and G325E was significantly impaired, and mutant P568L was impaired to a lesser extent. The remaining mutants were not significantly impaired.

(c) Growth defects of *ded1-1D5* cells correlate with lower expression of Cig2 according to immunoblotting of the HA epitope tagged Cig2.

(d) The decrease in expression is not due to lower mRNA levels as indicated by qRT-PCR of *cig2⁺* transcripts normalized to *adh1⁺*.

Table S1. Crystallographic statistics.

| | <i>HsDDX3X (135-582)</i> D354V | <i>HsDDX3X (135-407)</i> |
|-------------------------------------|--|---------------------------|
| Data collection | | |
| Space group | P4 ₃ 2 ₁ 2 | P3 ₁ |
| Cell dimensions | | |
| <i>a, b, c</i> (Å) | 105.755, 105.755, 152.633 | 75.637, 75.637, 121.388 |
| α, β, γ (°) | 90, 90, 90 | 90, 90, 120 |
| Resolution (Å) | 50-3.20 (3.31-3.20) | 50-2.30 (2.38-2.30) |
| R_{sym} | 0.128 (0.641) | 0.088 (0.577) |
| $I / \sigma I$ | 37.2 (5.7) | 27.0 (2.3) |
| Completeness (%) | 100 (100) | 99.6 (100) |
| Redundancy | 14.0 (14.6) | 3.8 (4.0) |
| Refinement | | |
| Resolution (Å) | 50-3.20 (3.31-3.20) | 50-2.30 (2.38-2.30) |
| No. reflections / Free | 14843/718 (1338/83) | 34116/1755 (3061/160) |
| $R_{\text{work}} / R_{\text{free}}$ | 0.206/0.271 (0.282/0.377) | 0.255/0.285 (0.386/0.426) |
| No. atoms | | |
| Protein | 3496 | 6265 |
| ADP | 27 | 81 |
| ion | 25 | 0 |
| Water | 0 | 0 |
| <i>B</i> -factors | | |
| Protein | 96.67 | 70.86 |
| ADP | 107.34 | 93.71 |
| ion | 146.75 | N/A |
| Water | N/A | N/A |
| R.m.s. deviations | | |
| Bond lengths (Å) | 0.008 | 0.007 |
| Bond angles (°) | 1.5 | 1.3 |

Table S2. Chemical Shift values for DDX3X domain D1 (in ppm) at 298 K.

| Residue | H | N | CA | CB |
|---------|------|--------|-------|-------|
| 128 | 8.25 | 109.09 | 44.76 | |
| 129 | 7.91 | 121.03 | 54.53 | 41.36 |
| 130 | 8.1 | 123.65 | 52.54 | 40.69 |
| 133 | 8.16 | 108.49 | 44.83 | |
| 134 | 8.6 | 122.18 | 56.91 | 65.12 |
| 137 | 8.31 | 112.52 | 59.47 | 64.74 |
| 138 | 7.23 | 123.52 | 52.2 | 31.58 |
| 140 | 8.63 | 124.62 | 52.98 | 39.51 |
| 143 | 8.77 | 113.86 | 55.57 | 64.32 |
| 145 | 8.33 | 118.21 | 58.43 | 28.45 |
| 146 | 7.41 | 120.37 | 56.68 | 40.54 |
| 147 | 8.32 | 118.6 | 59.64 | 28.18 |
| 148 | 7.78 | 116.77 | 58.01 | 27.14 |
| 149 | 7.43 | 118.65 | 58.22 | 29.29 |
| 150 | 8.11 | 115.99 | 56.11 | |
| 151 | 7.56 | 112.61 | 57.04 | 38.25 |
| 152 | 7.46 | 114.8 | 59.12 | 63.49 |
| 153 | 8.43 | 110.18 | 44.91 | |
| 154 | 8.14 | 108.04 | 44.76 | |
| 156 | 8.13 | 113.63 | 61.66 | 69.39 |
| 157 | 8.4 | 110.68 | 44.98 | |
| 158 | 7.82 | 119.68 | 60.7 | 37.88 |
| 159 | 8.33 | 122.03 | 52.46 | 38.25 |
| 160 | 8.21 | 121.22 | 58.01 | 38.69 |

| | | | | |
|-----|------|--------|-------|-------|
| 161 | 8.26 | 121.27 | 56.66 | 29.07 |
| 162 | 7.84 | 119.93 | 55.87 | 31.88 |
| 163 | 8.05 | 119.92 | 57.23 | 37.89 |
| 164 | 8 | 120.96 | 54.73 | 40.77 |
| 165 | 8.31 | 119.3 | 53.64 | 39.95 |
| 166 | 7.31 | 121.81 | 57.72 | 38.02 |
| 168 | 7.91 | 120.33 | 60.53 | 33.99 |
| 169 | 8.31 | 125.84 | 54.46 | 32.1 |
| 170 | 8.64 | 128.87 | 50.24 | 21.14 |
| 171 | 9.46 | 116.68 | 60.75 | 71.19 |
| 172 | 8.38 | 111.8 | 43.73 | |
| 173 | 8.84 | 118.05 | 52.61 | 38.62 |
| 175 | 8.55 | 120.34 | 57.57 | 26.92 |
| 178 | 7.57 | 116.1 | 55.87 | 27.96 |
| 179 | 8.09 | 112.33 | 59.42 | 38.77 |
| 180 | 8.28 | 115.05 | 55.57 | 30.55 |
| 181 | 7.79 | 113.27 | 55.13 | 64.9 |
| 182 | 8.85 | 123.59 | 61.63 | 36.99 |
| 184 | 7.64 | 120.6 | 56.16 | 40.8 |
| 185 | 7.29 | 112.15 | 58.53 | 33.58 |
| 186 | 8.46 | 122.52 | 55.72 | 27.96 |
| 187 | 8.44 | 122.26 | 55.42 | 34.32 |
| 188 | 8.72 | 110.3 | 44.3 | |
| 189 | 8.37 | 117.08 | 59.12 | 30.1 |
| 190 | 8.04 | 120.64 | 65.39 | 36.48 |
| 191 | 8.81 | 118.17 | 61.5 | |

| | | | | |
|-----|------|--------|-------|-------|
| 192 | 8.3 | 114.11 | 56.78 | 28.18 |
| 193 | 7.91 | 107.24 | 46.39 | |
| 194 | 7.85 | 122 | 55.35 | 37.8 |
| 195 | 8.89 | 123.47 | 65.32 | |
| 196 | 7.33 | 119.12 | 58.94 | |
| 197 | 7.28 | 119.15 | 56.94 | 39.36 |
| 198 | 7.57 | 109.08 | 62.9 | 69.86 |
| 199 | 7.51 | 112.65 | 56.83 | |
| 200 | 7.64 | 120.07 | 56.19 | 36.28 |
| 201 | 8.4 | 112.79 | 62.68 | 68.82 |
| 202 | 7.92 | 120.37 | 52.63 | 30.56 |
| 204 | 8.01 | 113.55 | 59.6 | 67.27 |
| 206 | 9.06 | 113.86 | 65.3 | 30.03 |
| 207 | 6.99 | 120.52 | 58.58 | 26.66 |
| 208 | 8.67 | 116.12 | 59.21 | 32.03 |
| 209 | 7.01 | 111.58 | 57.13 | 32.44 |
| 210 | 8.88 | 118.16 | 54.46 | 18.18 |
| 211 | 8.1 | 113.92 | 68.18 | |
| 213 | 6.54 | 116.33 | 66.03 | 38.17 |
| 214 | 8.12 | 118.65 | 64.73 | |
| 216 | 7.25 | 115.8 | 55.51 | 28.1 |
| 217 | 8.06 | 113.99 | 56 | 27.73 |
| 218 | 7.41 | 117.05 | 50.99 | 27.96 |
| 220 | 7.58 | 120.26 | 52.82 | |
| 221 | 8.8 | 127.21 | 52.17 | 35.47 |
| 222 | 8.96 | 127.12 | 48.62 | 20.81 |

| | | | | |
|-----|------|--------|-------|-------|
| 223 | 8.92 | 123.49 | 56.13 | 27.07 |
| 224 | 7.82 | 125.43 | 50.24 | 20.77 |
| 225 | 8.81 | 118.52 | 54.39 | 29.58 |
| 230 | 7.68 | 121.29 | 59 | 30.62 |
| 231 | 7.45 | 111.15 | 64.83 | 66.68 |
| 232 | 8.2 | 120.98 | 54.01 | 16.85 |
| 233 | 7.08 | 114.98 | 54.32 | 17.07 |
| 234 | 6.6 | 102.55 | 56.08 | |
| 235 | 7.98 | 121.17 | 54.91 | |
| 236 | 7.83 | 120.87 | 52.17 | |
| 238 | 6.99 | 119.18 | 66.15 | 37.34 |
| 239 | 8.16 | 117.27 | 57.42 | 39.51 |
| 240 | 7.64 | 106.99 | 61.37 | 63.85 |
| 241 | 7.39 | 119.12 | 57.97 | 28.03 |
| 242 | 7.93 | 120.98 | 65.62 | |
| 243 | 8.55 | 117.74 | 56.88 | |
| 244 | 7.65 | 110.36 | 60.9 | 63.37 |
| 245 | 8.62 | 119.96 | 55.66 | 40.99 |
| 246 | 8.44 | 108.11 | 43.84 | |
| 248 | 8.3 | 110.29 | 44.8 | |
| 249 | 8.35 | 118.54 | 57.11 | |
| 251 | 7.45 | 117.71 | 56.42 | 40.39 |
| 252 | 7.5 | 118.85 | 58.61 | 28.84 |
| 253 | 7.63 | 120.28 | 53.42 | 17.8 |
| 254 | 7.63 | 117.13 | 56.82 | 31.66 |
| 255 | 7.9 | 119.71 | 57.35 | 31.55 |

| | | | | |
|-----|------|--------|-------|-------|
| 256 | 8.1 | 119.18 | 57.04 | 28.99 |
| 257 | 8.12 | 117.45 | 53.74 | 38.32 |
| 258 | 8.2 | 108.26 | 45.5 | |
| 259 | 8.35 | 120.06 | 56.83 | |
| 260 | 8.04 | 117.94 | 57.21 | 37.88 |
| 261 | 8.05 | 109.08 | 45.12 | |
| 263 | 8.21 | 121.7 | 56.18 | |
| 264 | 7.61 | 121.99 | 56.31 | 33.51 |
| 265 | 7.44 | 119.63 | 52.98 | 29.73 |
| 268 | 8.51 | 121.33 | 61.93 | |
| 269 | 7.65 | 109.58 | 54.89 | |
| 270 | 8.48 | 129.47 | 52.3 | |
| 271 | 9.3 | 126.04 | 59.24 | |
| 272 | 9.12 | 125.18 | 52.14 | 43.61 |
| 273 | 8.33 | 122.36 | 47.76 | |
| 275 | 6.41 | 99.66 | 57.21 | 72.62 |
| 276 | 8.89 | 121.6 | 58.66 | 29.06 |
| 277 | 8.72 | 115.63 | 60.16 | 27.51 |
| 278 | 7.62 | 119.33 | 56.46 | 40.69 |
| 279 | 8.19 | 120.22 | 54.75 | 15.69 |
| 280 | 8.61 | 115.57 | 66.7 | 30.59 |
| 281 | 7.44 | 119.72 | 59.04 | 27.75 |
| 282 | 8.5 | 120.09 | 65.15 | |
| 283 | 8.54 | 120.36 | 60.62 | 40.02 |
| 284 | 8.78 | 118.57 | 58.94 | 27.35 |
| 285 | 7.45 | 119.4 | 59.2 | 28.1 |

| | | | | |
|-----|-------|--------|-------|-------|
| 286 | 8.53 | 120.35 | 54.85 | 16.44 |
| 287 | 8.4 | 119.18 | 59.79 | 29.51 |
| 288 | 6.92 | 116.74 | 59.5 | |
| 289 | 7.29 | 109.83 | 59.76 | |
| 290 | 7.83 | 114.06 | 57.54 | 61.12 |
| 291 | 6.91 | 127.69 | 58.52 | |
| 292 | 8.07 | 116.08 | 58.43 | 26.03 |
| 293 | 8.09 | 114.38 | 56 | 68.02 |
| 294 | 8.25 | 117.41 | 55.11 | 28.09 |
| 295 | 7.98 | 119.65 | 61.79 | 31.49 |
| 296 | 11.64 | 134.65 | 54.45 | |
| 298 | 8.64 | 116.74 | 58.09 | 33.21 |
| 299 | 8.38 | 122.52 | 57.08 | 33.95 |
| 300 | 8.52 | 116.83 | 58.24 | 33.14 |
| 301 | 6.41 | 113.86 | 53.64 | 38.32 |
| 302 | 7.49 | 104.99 | 44.34 | |
| 306 | 8.84 | 128.43 | 64.01 | 37.88 |
| 307 | 8.21 | 111.68 | 46.91 | |
| 308 | 8.01 | 120.74 | 57.93 | 27.36 |
| 309 | 6.88 | 118.06 | 58.05 | 26.95 |
| 310 | 8.45 | 120.15 | 65.88 | 36.72 |
| 311 | 7.61 | 117.27 | 58.93 | 28.99 |
| 312 | 7.49 | 117.7 | 57.2 | 40.91 |
| 313 | 8.03 | 120.21 | 57.54 | 41.24 |
| 314 | 7.67 | 113.99 | 57.93 | 28.55 |
| 315 | 7.2 | 116.52 | 56.77 | 28.65 |

| | | | | |
|-----|------|--------|-------|-------|
| 316 | 7.64 | 109.5 | 43.73 | |
| 317 | 8.13 | 122.24 | 57.64 | 29.14 |
| 318 | 8.68 | 123.77 | 58.22 | 33.29 |
| 319 | 7.24 | 120.37 | 53.84 | 43.8 |
| 320 | 8.79 | 128.76 | 52.14 | 44.24 |
| 321 | 8.91 | 128.13 | 59.84 | |
| 322 | 9.34 | 127.13 | 49.76 | 24.25 |
| 323 | 6.94 | 108.75 | 57.94 | 66.61 |
| 325 | 7.6 | 103.77 | 46.93 | |
| 326 | 7.4 | 122.12 | 54.72 | 26.18 |
| 327 | 7.66 | 119.15 | 57.54 | 38.84 |
| 328 | 7.71 | 118.47 | 66.75 | 30.1 |
| 329 | 7.58 | 118.83 | 57.24 | 40.62 |
| 330 | 7.83 | 115.15 | 57.66 | |
| 331 | 8.57 | 121.15 | 59.11 | |
| 332 | 8.88 | 121.87 | 58.8 | 28.62 |
| 333 | 7.48 | 114.9 | 55.6 | 30.18 |
| 334 | 7.86 | 107.61 | 45.8 | |
| 335 | 7.86 | 112.3 | 54 | 31.52 |
| 336 | 6.68 | 115.77 | 55.93 | 40.62 |
| 337 | 8.69 | 112.46 | 43.13 | |
| 338 | 8.85 | 122.84 | 54.16 | 39.58 |
| 339 | 9.44 | 112.83 | 55.31 | 38.62 |
| 340 | 8.49 | 113.19 | 55.05 | 38.62 |
| 341 | 7.4 | 121.86 | 59.63 | 38.54 |
| 342 | 8.21 | 125.81 | 55.67 | 33.36 |

| | | | | |
|-----|------|--------|-------|-------|
| 343 | 7.81 | 116.87 | 55.89 | |
| 344 | 9.13 | 126.71 | 52.63 | 43.5 |
| 345 | 9.08 | 125.94 | 59.44 | 33.21 |
| 346 | 8.77 | 126.08 | 54.59 | 41.81 |
| 347 | 8.77 | 124.37 | 52.39 | 42.13 |
| 348 | 7.97 | 118.43 | 56.77 | 26.77 |
| 349 | 8.93 | 118.61 | 55.65 | 17.74 |
| 350 | 8.89 | 113.49 | 55.79 | 36.91 |
| 351 | 7.92 | 123.99 | 58.32 | 28.77 |
| 352 | 8.39 | 114.95 | 60.83 | 33.21 |
| 353 | 7.96 | 118.52 | 57.87 | 38.67 |
| 354 | 8.51 | 123.69 | 57.11 | 40.25 |
| 355 | 7.84 | 115.02 | 56.29 | 32.92 |
| 356 | 7.64 | 105.14 | 45.39 | |
| 357 | 7.71 | 113.04 | 56.61 | 38.17 |
| 358 | 9.4 | 122.8 | 62.52 | 25.73 |
| 360 | 7.7 | 117.02 | 60.01 | 27.29 |
| 361 | 8.57 | 117.33 | 65.57 | 36.84 |
| 362 | 8.76 | 118.05 | 60.77 | 28.03 |
| 363 | 7.76 | 121.27 | 58.53 | |
| 364 | 7.73 | 116.77 | 64.6 | 38.54 |
| 365 | 8.07 | 114.52 | 64.68 | 32.47 |
| 366 | 8.4 | 114.96 | 56.55 | 31.29 |
| 367 | 6.93 | 115.14 | 54.69 | 28.25 |
| 368 | 8.24 | 128.37 | 53.28 | 44.39 |
| 369 | 9.86 | 114.43 | 60.75 | 68.9 |

| | | | | |
|-----|-------|--------|-------|-------|
| 370 | 7.93 | 123.02 | 54.13 | 33.43 |
| 373 | 8.46 | 120.19 | 56.97 | 31.65 |
| 374 | 8.66 | 113.68 | 45.11 | |
| 375 | 7.61 | 121.02 | 64.65 | 30.92 |
| 379 | 9.03 | 123.84 | 53.21 | 40.17 |
| 380 | 9 | 121.55 | 53.94 | 36.91 |
| 381 | 8.93 | 121.27 | 55.38 | 42.39 |
| 382 | 8.72 | 114.9 | 57.12 | 66.08 |
| 383 | 8.75 | 128.31 | 54.2 | 18.73 |
| 384 | 7.67 | 105.74 | 59.57 | 72.07 |
| 388 | 9.78 | 116.24 | 59.94 | 27.51 |
| 389 | 6.89 | 119.05 | 59.43 | 34.25 |
| 390 | 7.51 | 121.18 | 58.83 | 25.96 |
| 391 | 8.03 | 117.05 | 57.42 | |
| 392 | 6.98 | 120.62 | 57.25 | 41.21 |
| 393 | 8.49 | 119.59 | 54.46 | 16.48 |
| 394 | 7.46 | 115.99 | 58.13 | 28.7 |
| 395 | 7.65 | 116.08 | 56.36 | 39.73 |
| 396 | 8.69 | 118.12 | 56.02 | 38.47 |
| 397 | 7.98 | 115.9 | 53.05 | 42.91 |
| 398 | 10.57 | 124.59 | 52.66 | 44.84 |
| 399 | 8.72 | 125.62 | 55.51 | 27.14 |
| 400 | 7.06 | 114.29 | 56.42 | 40.54 |
| 401 | 8.49 | 121.52 | 58.56 | 37.73 |
| 402 | 8.9 | 129.34 | 55.46 | 40.64 |
| 403 | 8.42 | 128.4 | 51.81 | 45.87 |

| | | | | |
|-----|------|--------|-------|-------|
| 404 | 8.74 | 126.37 | 50.27 | 19.89 |
| 405 | 8.21 | 123.74 | 61.12 | 31.51 |
| 406 | 8.81 | 116.23 | 44.84 | |
| 407 | 7.84 | 123.9 | 56.88 | 30.84 |

Table S3. Yeast strains used in this study.

| Name | Description |
|-------------------|---|
| PY 7803 (673)* | <i>ded1-61 cig2-HA leu1-32</i> |
| PY 7805 (669)* | <i>ded1-1D5 cig2-HA</i> |
| PY 7885 | <i>ded1-1D5 cig2-HA leu1-32</i> |
| PY 8049/50 | <i>ded1-1D5 cig2-HA leu1-32 + JP2102 [pREP41-V5-Ded1]</i> |
| PY 8053/54 | <i>ded1-1D5 cig2-HA leu1-32 + JP2104 [pREP41-V5-DDX3]</i> |
| PY 8108/09 | <i>ded1-1D5 cig2-HA leu1-32 + JP2116 [pREP41-V5-DDX3 G302V]</i> |
| PY 8111/12 | <i>ded1-1D5 cig2-HA leu1-32 + JP2132 [pREP41-V5-DDX3 A222P]</i> |
| PY 8115/16 | <i>ded1-1D5 cig2-HA leu1-32 + JP2133 [pREP41-V5-DDX3 G325E]</i> |
| PY 8119/20 | <i>ded1-1D5 cig2-HA leu1-32 + JP2134 [pREP41-V5-DDX3 T275M]</i> |
| PY 8123/24 | <i>ded1-1D5 cig2-HA leu1-32 + JP2135 [pREP41-V5-DDX3 R351W]</i> |
| PY 8127/28 | <i>ded1-1D5 cig2-HA leu1-32 + JP2136 [pREP41-V5-DDX3 P568L]</i> |
| PY 8131/32 | <i>ded1-1D5 cig2-HA leu1-32 + JP2137 [pREP41-V5-DDX3 L353F]</i> |
| PY 8135/36 | <i>ded1-1D5 cig2-HA leu1-32 + JP2138 [pREP41-V5-DDX3 K230A]</i> |
| PY 8139/40 | <i>ded1-1D5 cig2-HA leu1-32 + JP2140 [pREP41-V5-DDX3 D354V]</i> |
| PY 8183/84 | <i>ded1-1D5 cig2-HA leu1-32 + JP2139 [pREP41-V5-DDX3 M370R]</i> |
| PY8393/8430 | <i>ded1-61 cig2-HA leu1-32 + JP1340 [pREP41-V5]</i> |
| PY 8397/98 | <i>ded1-61 cig2-HA leu1-32 + JP2104 [pREP41-V5-DDX3]</i> |
| PY 8400/01 | <i>ded1-61 cig2-HA leu1-32 + JP2116 [pREP41-V5-DDX3 G302V]</i> |
| PY 8403/04 | <i>ded1-61 cig2-HA leu1-32 + JP2132 [pREP41-V5-DDX3 A222P]</i> |
| PY 8406/07 | <i>ded1-61 cig2-HA leu1-32 + JP2133 [pREP41-V5-DDX3 G325E]</i> |
| PY 8409/10 | <i>ded1-61 cig2-HA leu1-32 + JP2134 [pREP41-V5-DDX3 T275M]</i> |
| PY 8412/13 | <i>ded1-61 cig2-HA leu1-32 + JP2135 [pREP41-V5-DDX3 R351W]</i> |

| | |
|------------|--|
| PY 8415/16 | <i>ded1-61 cig2-HA leu1-32 + JP2136 [pREP41-V5-DDX3 P568L]</i> |
| PY 8418/19 | <i>ded1-61 cig2-HA leu1-32 + JP2137 [pREP41-V5-DDX3 L353F]</i> |
| PY 8421/22 | <i>ded1-61 cig2-HA leu1-32 + JP2138 [pREP41-V5-DDX3 K230A]</i> |
| PY 8424/25 | <i>ded1-61 cig2-HA leu1-32 + JP2139 [pREP41-V5-DDX3 M370R]</i> |
| PY 8427/28 | <i>ded1-61 cig2-HA leu1-32 + JP2140 [pREP41-V5-DDX3 D354V]</i> |

* Published in Grallert. et al. [4]

Table S4. List of Plasmids used in this study

| Plasmid | Description |
|---------|--|
| pLE193 | His ₆ -DDX3X(135-582) |
| pLE194 | His ₆ -DDX3X(168-582) |
| pLE210 | His ₆ -DDX3X(135-582) G302V |
| pLE224 | His ₆ -DDX3X(135-582) L353F |
| pLE228 | His ₆ -DDX3X(135-582) G325E |
| pLE230 | His ₆ -DDX3X(135-582) D354V |
| pLE231 | His ₆ -DDX3X(135-407) |
| pLE235 | His ₆ -DDX3X(408-582) |
| JP1340 | pREP41-3x-V5 |
| JP2102 | pREP41-3x-V5- <i>ded1</i> ⁺ |
| JP2104 | pREP41-3x-V5-DDX3X |
| JP2115 | pREP41-3x-V5-DDX3X G302V |
| JP2132 | pREP41-3x-V5-DDX3X A222P |
| JP2133 | pREP41-3x-V5-DDX3X G325E |
| JP2134 | pREP41-3x-V5-DDX3X T275M |
| JP2135 | pREP41-3x-V5-DDX3X R351W |
| JP2136 | pREP41-3x-V5-DDX3X P568L |
| JP2137 | pREP41-3x-V5-DDX3X L353F |
| JP2138 | pREP41-3x-V5-DDX3X K230A |
| JP2139 | pREP41-3x-V5-DDX3X M370R |
| JP2140 | pREP41-3x-V5-DDX3X D354V |

Supplementary References

- [1] Sengoku T, Nureki O, Nakamura A, Kobayashi S, Yokoyama S. Structural basis for RNA unwinding by the DEAD-box protein Drosophila Vasa. *Cell*. 2006;125:287-300.
- [2] Luo D, Ding SC, Vela A, Kohlway A, Lindenbach BD, Pyle AM. Structural insights into RNA recognition by RIG-I. *Cell*. 2011;147:409-22.
- [3] Mallam AL, Del Campo M, Gilman B, Sidote DJ, Lambowitz AM. Structural basis for RNA-duplex recognition and unwinding by the DEAD-box helicase Mss116p. *Nature*. 2012;490:121-5.
- [4] Grallert B, Kearsey SE, Lenhard M, Carlson CR, Nurse P, Boye E, et al. A fission yeast general translation factor reveals links between protein synthesis and cell cycle controls. *J Cell Sci*. 2000;113 (Pt 8):1447-58.